Available on CMS information server

CMS NOTE 2006/139

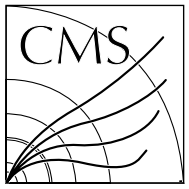

The Compact Muon Solenoid Experiment

CMS Note

Mailing address: CMS CERN, CH-1211 GENEVA 23, Switzerland

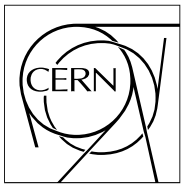

1 May 2007

Synchronization and Timing in CMS HCAL

CMS HCAL Collaboration

G. Baiatian, A. Sirunyan

Yerevan Physics Institute, Yerevan, Armenia

I. Emeliantchik, V. Massolov, N. Shumeiko, R. Stefanovich

NCPHEP, Minsk, Belarus

J. Damgov, L. Dimitrov, V. Genchev, S. Piperov, I. Vankov

Institute for Nuclear Research and Nuclear Energy, Bulgarian Academy of Science, Sofia, Bulgaria

L. Litov

Sofia University, Sofia, Bulgaria

G. Bencze, A. Laszlo, A. Pal, G. Vesztergombi, P. Zalan

KFKI-RMKI, Research Institute for Particle and Nuclear Physics, Budapest, Hungary

A. Fenyvesi

ATOMKI, Debrecen, Hungary

H. Bawa, S. Beri, V. Bhatnagar, M. Kaur, J. Kohli, A. Kumar, J. Singh

Panjab University, Chandigarh, 160 014, India

B. Acharya, Sud. Banerjee, Sun. Banerjee, S. Chendvankar, S. Dugad, S. Kalmani, S. Katta, K. Mazumdar, N. Mondal, P. Nagaraj, M. Patil, L. Reddy, B. Satyanarayana, S. Sharma, K. Sudhakar, P. Verma

Tata Institute of Fundamental Research, Mumbai, India

M. Hashemi[1)], M. Mohammadi-Najafabadi[2)], S. Paktinat[3)]

Institute for Studies in Theoretical Physics and Mathematics, Tehran, Iran

I. Golutvin, V. Kalagin, I. Kosarev, V. Ladygin, G. Mescheryakov, P. Moissenz, A. Petrosyan, S. Sergeyev, V. Smirnov, A. Vishnevskiy, A. Volodko, A. Zarubin

[1)] Also at Sharif University of Technology, Tehran, Iran.

[2)] Also at Sharif University of Technology, Tehran, Iran.

[3)] Also at Sharif University of Technology, Tehran, Iran.

JINR, Dubna, Russia

V. Gavrilov, Y. Gershtein[4)], N. Ilyina, V. Kaftanov, I. Kisselevich, V. Kolossov, A. Krokhotin, S. Kuleshov, D. Litvintsev[5)], A. Ulyanov, G. Safronov, S. Semenov, V. Stolin

ITEP, Moscow, Russia

A. Demianov, A. Gribushin, O. Kodolova, S. Petrushanko, L. Sarycheva, V. Teplov, I. Vardanyan, A. Yershov

Moscow State University, Moscow, Russia

V. Abramov, P. Goncharov, A. Kalinin, A. Khmelnikov, A. Korablev, Y. Korneev, A. Krinitsyn, V. Kryshkin, V. Lukanin, V. Pikalov, A. Ryazanov, V. Talov, L. Turchanovich, A. Volkov

IHEP, Protvino, Russia

T. Camporesi, T. de Visser, E. Vlassov[6)]

CERN, Geneva, Switzerland

S. Aydin, M. Bakirci, S. Cerci, I. Dumanoglu, E. Eskut, A. Kayis-Topaksu, S. Koylu, P. Kurt, G. Onengut, H. Ozkurt, A. Polatoz, K. Sogut, H. Topakli, M. Vergili, T. Yetkin

Cukurova University, Adana, Turkey

K. Cankoçak[7)], A. Esendemir, H. Gamsizkan, M. Guler, C. Ozkan, S. Sekmen, M. Serin-Zeyrek, R. Sever, E. Yazgan, M. Zeyrek

Middle East Technical University, Ankara, Turkey

M. Deliomeroglu, E. Gülmez, E. Isiksal[8)], M. Kaya[9)], S. Ozkorucuklu[10)]

Bogazici University, Istanbul, Turkey

L. Levchuk, P. Sorokin

KIPT, Kharkov, Ukraine

V. Senchyshyn

Institute for Scintillation Materials NASU, Kharkov, Ukraine

J. Hauptman

Iowa State University, Ames, IA, USA

S. Abdullin, J. Elias, D. Elvira, J. Freeman, D. Green, S. Los, V. O'Dell, A. Ronzhin, I. Suzuki, R. Vidal, J. Whitmore

Fermi National Accelerator Laboratory, Batavia, IL, USA

M. Arcidy, E. Hazen, A. Heering, C. Lawlor, D. Lazic, E. Machado, J. Rohlf, F. Varela, S. X. Wu

Boston University, Boston, MA, USA

D. Baden, R. Bard, S. Eno, T. Grassi, C. Jarvis, R. Kellogg, S. Kunori, J. Mans[11)], A. Skuja

---

[4)] Now at Florida State University, Tallahassee, FL, USA.

[5)] Now at FNAL, Batavia, IL, USA.

[6)] Also with ITEP, Moscow, Russia.

[7)] At Mugla University, Mugla, Turkey.

[8)] At Marmara University, Istanbul, Turkey.

[9)] At Kafkas University, Kars, Turkey.

[10)] At Süleyman Demirel University, Isparta, Turkey.

[11)] Now at University of Minnesota, Minneapolis, MN, USA.

University of Maryland, College Park, MD, USA

V. Podrasky, C. Sanzeni, D. Winn

Fairfield University, Fairfield, CT, USA

U. Akgun, S. Ayan, F. Duru, J. Merlo, A. Mestvirishvili, M. Miller, E. Norbeck, J. Olson, Y. Onel, I. Schmidt

University of Iowa, Iowa City, IA, USA

N. Akchurin, K. Carrell, K. Gümüş, H. Kim, M. Spezziga, R. Thomas, R. Wigmans

Texas Tech University, Lubbock, TX, USA

M. Baarmand, H. Mermerkaya, R. Ralich, I. Vodopiyanov

Florida Institute of Technology, Melbourne, FL, USA

L. Kramer, S. L. Linn, P. Markowitz

Florida International University, Miami, FL, USA

P. Cushman, Y. Ma, B. Sherwood

University of Minnesota, Minneapolis, MN, USA

L. Cremaldi, J. Reidy, D. A. Sanders

University of Mississippi, Oxford, MS, USA

D. Karmgard, R. Ruchti

University of Notre Dame, Notre Dame, IN, USA

W. Fisher, C. Tully

Princeton University, Princeton, NJ, USA

A. Bodek, P. de Barbaro, H. Budd, Y. Chung, T. Haelen

University of Rochester, Rochester, NY, USA

S. Hagopian, V. Hagopian, K. Johnson

Florida State University, Tallahassee, FL, USA

V. Barnes, A. Laasanen

Purdue University, West Lafayette, IN, USA

Abstract

The synchronization and timing of the hadron calorimeter (HCAL) for the Compact Muon Solenoid has been extensively studied with test beams at CERN during the period 2003-4, including runs with 40 MHz structured beam. The relative phases of the signals from different calorimeter segments are timed to 1 ns accuracy using a laser and equalized using programmable delay settings in the front-end electronics. The beam was used to verify the timing and to map out the entire range of pulse shapes over the 25 ns interval between beam crossings. These data were used to make detailed measurements of energy-dependent time slewing effects and to tune the electronics for optimal performance.

1 Introduction

The hadron calorimeter (HCAL) [1, 2, 3, 4, 5] for the Compact Muon Solenoid (CMS) detector [6] is designed to measure energy deposits resulting from pp collisions at 40.079 MHz at the Large Hadron Collider (LHC) [7]. Thorough understanding of the synchronization and timing of the detector is essential in order to indentify each energy deposit with the proper beam crossing. All sub-components of HCAL, barrel wedges (HB), endcap wedges (HE), forward wedges (HF), and outer scintillators (HO) have been extensively studied in CERN test beams using beams of pions, electrons, and muons of varying energies. The hardware set up in the H2 test beam at CERN is described in [2, 3, 4, 5]. Special runs were taken in 2003 and 2004 with structured beam in which protons were delivered with a 25 ns spacing in order to emulate the LHC crossing frequency.

2 HCAL Readout Control System

The application specific integrated circuit (ASIC) for the HCAL front-end electronics (QIE) is described in [8]. The front-end boards consist of six QIEs which are controlled by three Channel Control ASICs (CCAs). Digitized data are fed into two gigabit optical link ASICs (GOLs) that drive vertical cavity surface emitting lasers (VCSELs) such that only two optical fibers are needed to transfer the data from the six channel readout board to the data acquisition system. The CCA [9] is a custom ASIC developed at FERMILAB whose basic functions are to supply clocks for QIEs with individually programmable delays, to align the data received from QIEs and to send the data to the GOL chips. Other CCA functions are to provide a serial interface for programming the CCA, to adjust QIE pedestal values, to set QIEs to fixed or auto ranging modes (for calibration or physics), and to issue resets, test patterns and test pulse triggers. Control of the front-end cards as well as delivery of clock and Trigger Timing Control (TTC) signals is performed through a Clock and Control Module (CCM) [10] that communicates with the detector control system (DCS) through an optically isolated RS 422 interface.

3 Synchronization Procedure

Synchronization of the HB wedges at the point of reception of the GOL data is achieved by cutting the digital optical fibers that transmit digitized data from the front end cards to the same length. The checks of the relative timing of signals from different ϕ sectors of two detector towers have shown that they are synchronized to within 0.2 ns. An additional equalization across η towers is necessary, however, because the analog signals travel different lengths along optical waveguides before reaching the photodetectors which are located on the ends of the wedges [2]. This effect is partially compensated by the time of flight of particles between the interaction point and the tower. Particles entering the detector at low $|\eta|$ have shorter times of flight, but the produced light has a longer distance to travel through optical waveguides. For the high $|\eta|$ towers the time of flight is longer, but the transmission time through the wave-guides is shorter. This compensation is not complete and there is still a need to adjust front-end delays so that all signals arrive at the hybrid photodiode (HPD) photo-detector input at the same time.

A laser calibration system was used to measure the relative time delay of signals from different (η, ϕ) towers. During the construction of the scintillators, the fibers that inject laser light into selected layers of the calorimeter have been cut so that the relative time of light injection into towers corresponds to the relative times of arrival of particles. By measuring the timing distribution of laser induced signals, we measure a distribution of mean arrival times that varies by several ns along the length of a wedge. A direct comparison of the laser pulses with the beam shows that they give the same timing which means we can set the timing of wedges not exposed to the test beam with confidence. Adjusting delays for each individual tower can be done in steps of 1 ns by programming the corresponding CCA. Checking that the delays are properly set was performed by sending electrons into each η tower of a given ϕ sector of the calorimeter, and the results are shown in Figure 1.

4 QIE Pulse Shape

After adjusting the relative delays of the (η, ϕ) towers, we performed a set of measurements where the adjusted delays were incremented in steps of 1 ns. The obtained time distributions are shown in Figure 2 using RF structured beam data. The horizontal axis is time in units of the 25 ns readout (called time sample below). The vertical axis is the linearized response in fC. For LHC operation, it will be necessary to record 5-6 time samples in order to record the complete energy deposit and to estimate out-of-time pileup. The resulting 25 plots show the complete family of possible HCAL pulse phases, from which we have the option to select the operating point.

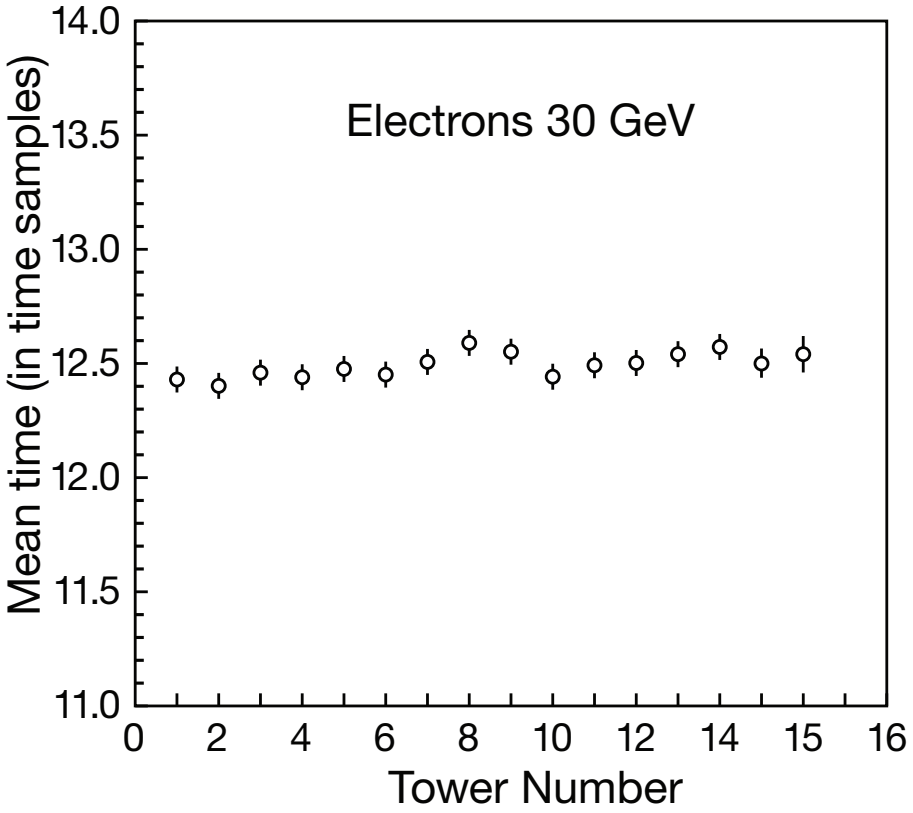

Figure 1: Mean signal arrival times in 25 ns units as a function of tower number (increasing $|\eta|$) for 30 GeV electrons after adjustments of delays as determined by a laser.

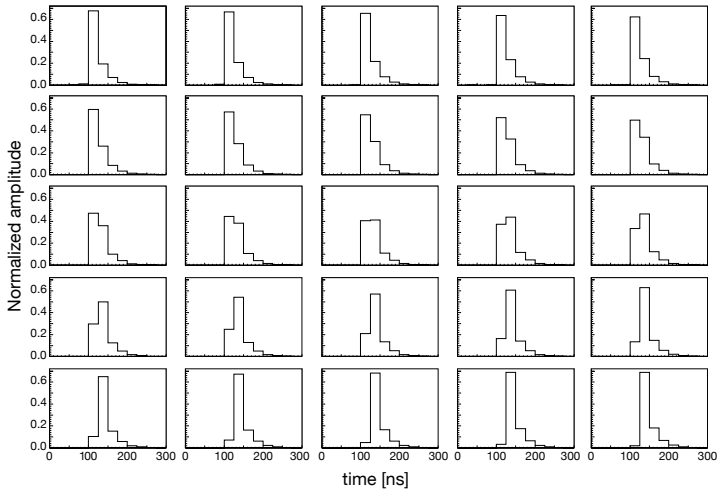

Figure 2: Energy deposited in a 300 ns interval with bins of 25 ns and with front-end electronics delays set in 25 increments of 1 ns each.

The QIE pulse shape has been studied extensively by using the phase adjusted data in 25 steps of 1 ns in order to a make a 1 ns deconvolution. Figure 3 shows the resulting pulse shapes for 30 GeV electrons and 300 GeV pions. The conclusion from this study is that the signal shape is stable for the energy range 30-300 GeV and doesn't show a significant difference due to the beam particle type. The pulse shape also agrees with that measured with a photo-multiplier tube and a 1 ns resolution digital scope [2].

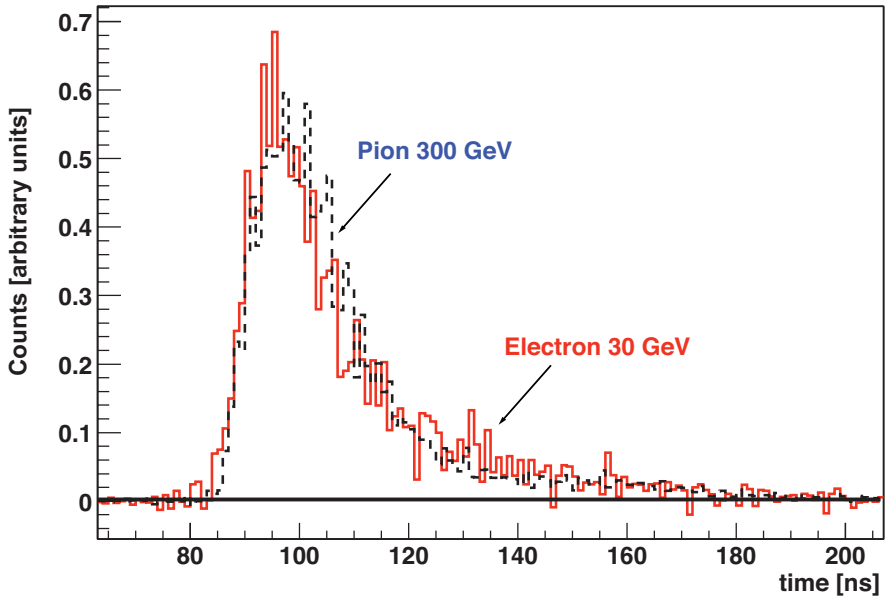

Figure 3: Pulse shape in 1 ns time bins for 30 GeV electrons and 300 GeV pions.

5 Phase Dependence of the Signal Amplitude

Another issue that was studied in detail during this period is a known time slewing of signals in the QIE. The data of Figure 3 already indicate that time slewing is not significant for energy deposits above 30 GeV. The requirement to minimize the noise of the system has led to the use of an intrinsically slow inverting amplifier with a dynamic input impedance. The outcome is that higher signals give a faster response time as shown on Fig. 4. The phase dependence of the signal amplitude was observed and measured directly on the QIE ASIC and compared with test beam data. Early measurements were optimized for low noise (3800e) which resulted in an unacceptably large time slewing (up to 16 ns).

After the 2003 test beam measurements, the time slewing was evaluated and adjusted on the bench. These results of this study are shown in Figure 5. The measurements showed that it was possible to substantially reduce the time slewing from 16 ns to a few ns while increasing the electronic noise only modestly. This is because the shot noise due to the input standing current depends on the square of the current while the time slewing had a much stronger current dependence. It was further observed that the inherent in the design of the QIE with four capacitor banks, the noise is correlated in adjacent time samples so that adding multiple time samples does not significantly increase noise. The time slewing labeled by "Noise 5420 e" was chosen for the HCAL production electronics. Note that muons, depositing about 2.5 GeV in HCAL will still have substantial time slew.

6 Energy Collection as a Function of the Number of Time Samples

The pulse width (Figure 2) and the time slew effect (Figure 5) put a strong limitation on the minimum number of the time slices which can be used for measurement of the energy deposited in a single tower. The upper limit on the number of time slices is defined in a large part by the presence of a large number of pileup events at the LHC. An average of nearly 20 pp interactions per bunch crossing occurs at design luminosity.

On the other hand, the time stability of the pulse shape allows potential usage of a smaller number of time samples because the uniform pulse shape allows a stable fractional energy collection for a fixed number of time samples and

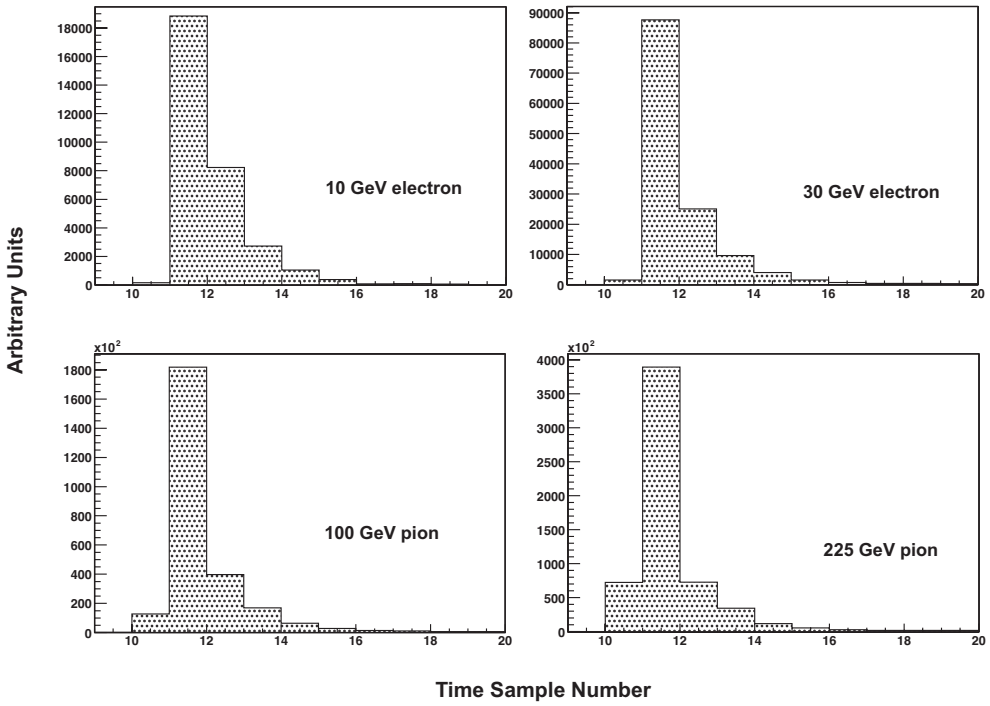

Figure 4: Pulse shape in 25 ns bins for 4 beam energies energy measured in the test beam (2003) before the time slewing adjustments.

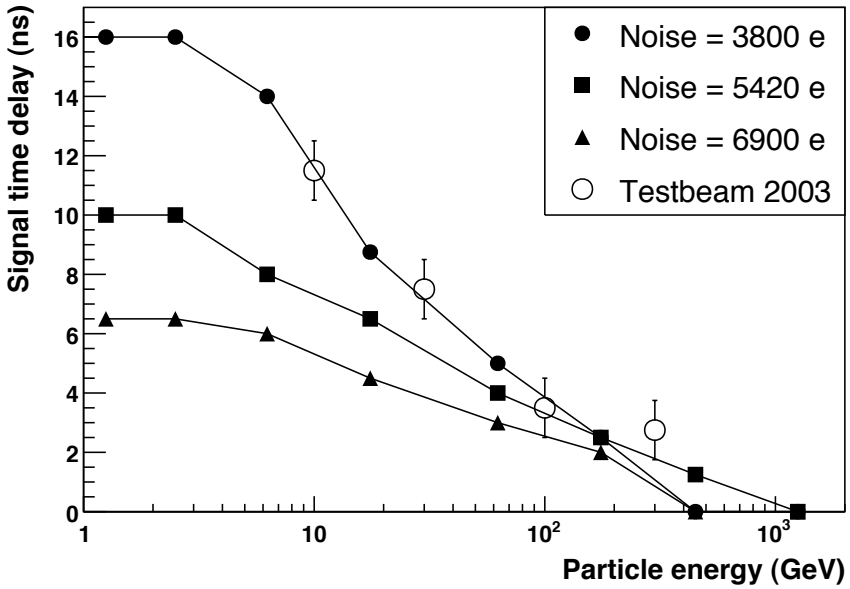

Figure 5: Time slewing *vs* beam energy for bench and test beam measurements.

phase. Figure 6 shows a correlation plot for normalized energy collection in one *vs* two consecutive time samples as a function of phase or time delay with respect to the start of the 25 ns bunch crossing cycle. The variation of the signal fraction in one time sample is 41-69%, while for two time slices it is much less, 77-88%. Figure 6 shows three transition regions. Points 1 and 25 (see Figure 2 for the pulse shapes), correspond to the case where the most energy is collected in a single sample. This is desirable for many reasons. However, because of the time slewing, it is not the most stable operating point. Point 13 corresponds to the pulse profile which has equal energy in two adjacent time samples. In this case, a single time sample has only 41% of the energy, a disadvantage for using a single bunch crossing to generate the level-1 (L1) trigger primitives (TPG). Point 19 corresponds to the pulse profile which has equal energy in the two time samples on either side of the time sample with the largest energy deposit. This is a stable region for the use of two time sample in the generation of the L1 TPG. Note that the data of Figure 5 can be used to correct the timing of low energy pulses. This correction will sharpen the particle passage time with respect to the bunch crossing time which will be useful in rejecting cosmic ray backgrounds.

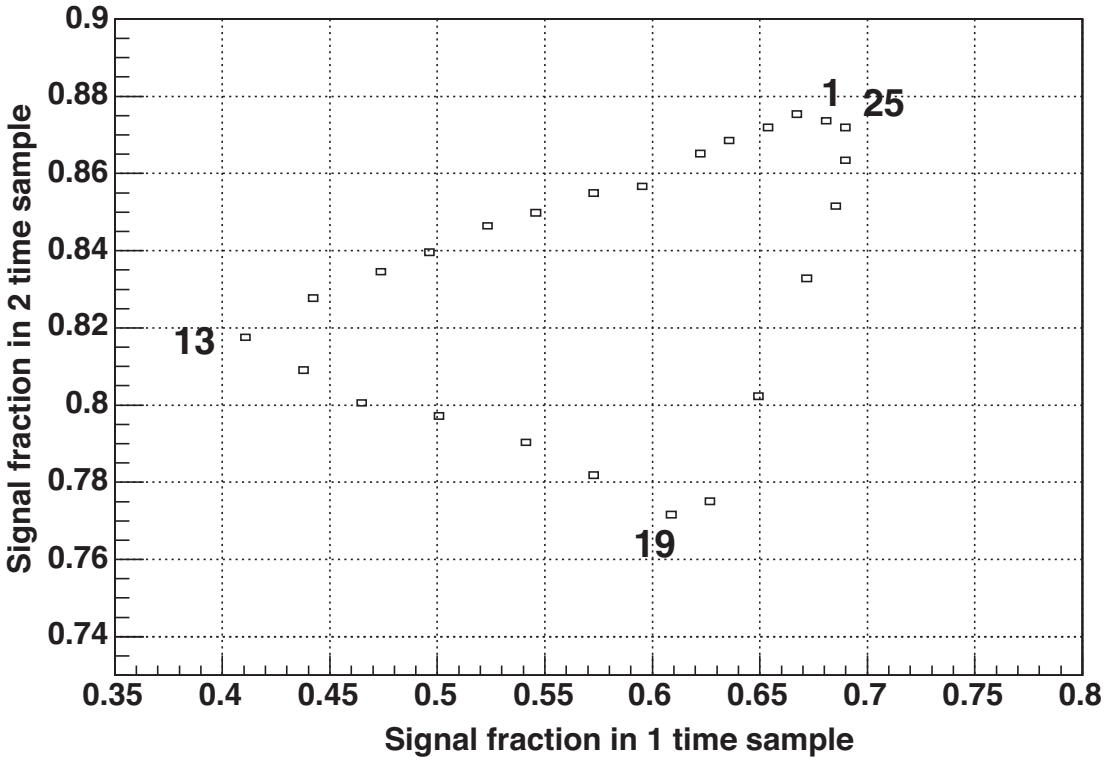

Figure 6: Energy fraction in two (vertical axis) *vs* one (horizontal axis) time sample. The phase step is 1 ns and the plot covers the complete 25 ns operational range within a single time sample.

7 Summary

The CMS HCAL data taken in the 2003-4 test beam with production electronics have allowed us to extensively test the operation of the control system for timing and synchronization. These data were used to map out the details of the HCAL pulse shape in 1 ns steps across the entire 25 ns beam crossing period. Detailed measurements of the time slewing as a function of deposited energy have allowed us to optimize performance so as to keep tight control of the synchronization without significantly increasing noise.

References

[1] *CMS The Hadron Calorimeter Technical Design Report*, CERN/LHCC 97-31 CMS TDR 2 (June 1997).

[2] G. Baiatian *et al*, Design, Performance, and Calibration of CMS Hadron-Barrel Calorimeter Wedges, CMS NOTE-2006/138.

[3] G. Baiatian *et al*, Design, Performance, and Calibration of CMS Hadron-Endcap Calorimeter Wedges, CMS Note in preparation (2006).

[4] G. Baiatian *et al*, Design, Performance, and Calibration of CMS Forward Calorimeter Wedges, CMS Note 2006/044.

[5] G. Baiatian *et al*, Energy Response and Longitudinal Shower Profiles Measured in CMS HCAL and Comparison With Geant4, CMS NOTE-2006/143.

[6] CMS Technical Proposal, CERN/LHCC 94-38, LHCC/P1 (December 1994).

[7] The LHC design report and current status is available at http://lhc-new-homepage.web.cern.ch/lhc-new-homepage/

[8] T. Zimmerman and J. R. Hoff, *The Design of a Charge-Integrating Modified Floating-Point ACD Chip*, IEEE J. Solid-State Circuits 39 (2004) 895.

[9] R. J. Yarema, A. Baumbaugh, A. Boubekeur, J. E. Elias, T. Shaw, *Channel Control ASIC for the CMS Hadron Calorimeter Front End Readout Module*, Proceedings of the Eight Workshop on Electronics for LHC Experiments, Colmar, France 2002.

[10] S. Holm, T. Shaw, J. Elias, S. Sergueev, *Design and Testing of a Radiation Tolerant Clock, Control and Monitor (CCM) Module for the CMS HCAL Electronics*, 2002 IEEE Nuclear Science Symposium and Medical Imaging Conference, Norfolk, VA USA, 2002.